



The University of
Nottingham

UNITED KINGDOM · CHINA · MALAYSIA

Puckett, Emily E. and Park, Jane and Combs, Matthew and Blum, Michael J. and Bryant, Juliet E. and Caccone, Adalgisa and Costa, Federico and Deinum, Eva E. and Esther, Alexandra and Himsworth, Chelsea G. and Keightley, Peter D. and Ko, Albert and Lundkvist, Åke and McElhinney, Lorraine M. and Morand, Serge and Robins, Judith and Russell, James and Strand, Tanja M. and Suarez, Olga and Yon, Lisa and Munshi-South, Jason (2016) Global population divergence and admixture of the brown rat (*Rattus norvegicus*). *Proceedings of the Royal Society B: Biological Sciences*, 283 (1841). 20161762/1-20161762/9. ISSN 1471-2954

Access from the University of Nottingham repository:

http://eprints.nottingham.ac.uk/37772/1/Puckett_etal-RatPhylogeog-bioarXiv.pdf

Copyright and reuse:

The Nottingham ePrints service makes this work by researchers of the University of Nottingham available open access under the following conditions.

This article is made available under the University of Nottingham End User licence and may be reused according to the conditions of the licence. For more details see:

http://eprints.nottingham.ac.uk/end_user_agreement.pdf

A note on versions:

The version presented here may differ from the published version or from the version of record. If you wish to cite this item you are advised to consult the publisher's version. Please see the repository url above for details on accessing the published version and note that access may require a subscription.

For more information, please contact eprints@nottingham.ac.uk

1
2
3
4
5
6
7
8
9
10
11
12
13
14
15
16
17
18
19
20
21
22
23
24
25
26
27
28
29
30
31
32
33
34
35
36
37
38
39
40
41
42
43
44
45
46

Title: Global population divergence and admixture of the brown rat (*Rattus norvegicus*)

Authors: Emily E. Puckett^{1*}, Jane Park¹, Matthew Combs¹, Michael J. Blum², Juliet E. Bryant³, Adalgisa Caccone⁴, Federico Costa⁵, Eva E. Deinum^{6,7}, Alexandra Esther⁸, Chelsea G. Himsworth⁹, Peter D. Keightley⁶, Albert Ko¹⁰, Åke Lundkvist¹¹, Lorraine M. McElhinney¹², Serge Morand¹³, Judith Robins^{14,15}, James Russell^{15,16}, Tanja M. Strand¹¹, Olga Suarez¹⁷, Lisa Yon¹⁸, and Jason Munshi-South^{1*}

¹- Louis Calder Center- Biological Field Station, Fordham University, Armonk, NY, USA

²- Xavier Center for Bioenvironmental Research, Tulane University, New Orleans, LA, USA

³- Oxford University Clinical Research Unit, Hanoi, Vietnam

⁴- Department of Ecology and Evolutionary Biology, Yale University, PO Box 208106, New Haven, CT 06520–8106, USA

⁵- Instituto de Saúde Coletiva, Universidade Federal da Bahia, Salvador, Brazil

⁶-University of Edinburgh, Institute of Evolutionary Biology, Ashworth Laboratories, Charlotte Auerbach Road, Edinburgh EH9 3FL, UK

⁷- Mathematical and Statistical Methods Group, Wageningen University, Droevendaalsesteeg 1, 6708 PB Wageningen, the Netherlands

⁸- Julius Kühn Institute, Federal Research Centre for Cultivated Plants, Institute for Plant Protection in Horticulture and Forests, Vertebrate Research, Münster, Germany

⁹- Animal Health Centre, British Columbia Ministry of Agriculture, 1767 Angus Campbell Road, Abbotsford, BC, Canada V3G 2M3

¹⁰- Laboratory of Epidemiology and Public Health, Yale University, New Haven, CT USA

¹¹-Department of Medical Biochemistry and Microbiology, Zoonosis Science Center, Uppsala University, Sweden

¹²-Wildlife Zoonoses and Vector Borne Disease Research Group, Animal and Plant Health Agency (APHA), Woodham Lane, New Haw, Surrey, UK

¹³- CNRS-CIRAD, Centre d'Infectiologie Christophe Mérioux du Laos, Vientiane, Lao PDR

¹⁴- Department of Anthropology, University of Auckland, Private Bag 92019, Auckland, New Zealand

¹⁵- School of Biological Sciences, University of Auckland, Private Bag 92019, Auckland, New Zealand

¹⁶- Department of Statistics, University of Auckland, Private Bag 92019, Auckland, New Zealand

¹⁷-Laboratorio de Ecología de Roedores Urbanos, IEGEBA-CONICET, EGE-Facultad de Ciencias Exactas y Naturales, Universidad de Buenos Aires Pabellon II, Ciudad Universitaria (C1428EHA), Buenos Aires, Argentina

¹⁸-School of Veterinary Medicine & Science, University of Nottingham, Sutton Bonington Campus, Loughborough, LE12 5RD, UK

***Corresponding Authors:**

Emily.E.Puckett@gmail.com (EEP) and jmunshisouth@fordham.edu (JM-S)

Keywords: commensal, invasive species, population genomics, cityscapes, phylogeography

47 **ABSTRACT**

48 Once restricted to northern China and Mongolia, the brown rat (*Rattus norvegicus*) now enjoys a
49 worldwide distribution due to the evolution of commensalism with humans. In contrast to black
50 rats and the house mouse, which have tracked the regional and global development of human
51 agricultural settlements, brown rats do not appear in the European historical record until the
52 1500s, suggesting their range expansion was a response to relatively recent increases in global
53 trade and modern sea-faring. We inferred the global phylogeography of brown rats using 32k
54 SNPs to reconstruct invasion routes from estimates of population divergence and admixture.
55 Globally, we detected 13 evolutionary clusters within five expansion routes. One cluster arose
56 following a southward expansion into Southeast Asia. Three additional clusters arose from two
57 independent eastward expansions: one expansion from Russia to the Aleutian Archipelago, and a
58 second to western North America. Rapid westward expansion resulted in the colonization of
59 Europe from which subsequent colonization of Africa, the Americas, and Australasia occurred,
60 and multiple evolutionary clusters were detected. An astonishing degree of fine-grained
61 clustering found both between and within our sampling sites underscored the extent to which
62 urban heterogeneity can shape the genetic structure of commensal rodents. Surprisingly, few
63 individuals were recent migrants despite continual global transport, suggesting that recruitment
64 into established populations is limited. Understanding the global population structure of *R.*
65 *norvegicus* offers novel perspectives on the forces driving the spread of zoonotic disease, and
66 yields greater capacity to develop targeted rat eradication programs.

67

68

69 INTRODUCTION

70 The development of agriculture and resultant transition from nomadic to sedentary human
71 societies created new ecological niches for species to evolve commensal or parasitic
72 relationships with humans (Jones, et al. 2013). The phylogeographic history of species living in
73 close association with people often mirrors global patterns of human exploration (Searle, et al.
74 2009; Gabriel, et al. 2015) and colonization (Matisoo-Smith and Robins 2004; Cucchi, et al.
75 2005; Suzuki, et al. 2013; Hulme-Beaman, et al. In Press). In particular, commensal rodent
76 distributions have been strongly influenced by the movement of humans around the world. Three
77 rodent species, the house mouse (*Mus musculus*), black rat (*Rattus rattus*), and brown rat (*R.*
78 *norvegicus*) are the most populous and successful invasive mammals, having colonized most of
79 the global habitats occupied by humans (Long 2003). The least is known about genomic
80 diversity and patterns of colonization in brown rats, including whether a history of
81 commensalism resulted in population divergence, and if so at what spatial scales. Our lack of
82 knowledge of the ecology and evolution of the brown rat is striking given that brown rats are
83 responsible for an estimated \$19 billion of damage annually (Pimentel, et al. 2000).
84 Understanding the evolutionary trajectories of brown rats is also a prerequisite to elucidating the
85 processes that resulted in a successful global invasion, including adaptations to a variety of
86 climates and anthropogenic stressors.

87
88 We inferred global routes of brown rat expansion, population differentiation, and admixture
89 using a dense, genome-wide nuclear dataset, a first for a commensal rodent (Lack, et al. 2012). A
90 previous mitochondrial study identified the center of origin (Song, et al. 2014) but did not
91 resolve relationships among invasive populations. That work, in combination with fossil
92 distributions (Smith and Xie 2008), suggested that brown rats originated in the colder climates of
93 northern China and Mongolia before expanding across central and western Asia, possibly
94 through human settlements associated with Silk Road trade routes. Based on historical records,
95 brown rats became established in Europe by the 1500s and were introduced to North America by
96 the 1750s (Armitage 1993). Brown rats now occupy nearly every major landmass (outside of
97 polar regions), and human-assisted colonization of islands remains a constant threat to insular
98 fauna (Harper and Bunbury 2015).

99

100 Commensalism has given rise to complex demographic and evolutionary scenarios in globally
101 distributed rodents. Although archaeological evidence indicates that commensalism arose long
102 after the emergence of sub-specific lineages in the house mouse in its native range of western
103 Asia (Prager, et al. 1998; Suzuki, et al. 2013), the geographic distribution of *M. m. domesticus*
104 mitochondrial haplotypes reflects transport by humans (Jones, et al. 2010; Suzuki, et al. 2013).
105 *M. m. domesticus* occurred in human settlements along the eastern Mediterranean Basin around
106 14 kya and rapidly colonized the western Mediterranean and central Europe approximately 3 kya
107 (Cucchi, et al. 2005). Both *M. m. musculus* and *M. m. castaneus* also exhibit regional
108 diversification of mitochondrial lineages due to natural range expansion and spread by human
109 transport (Suzuki, et al. 2013). Human mediated movement has also been implicated in the
110 creation of hybrid zones between subspecies in Scandinavia, China, and New Zealand (Jones, et
111 al. 2010; Jing, et al. 2014; King 2016). Similarly, geographically isolated lineages formed prior
112 to commensalism in the black rat species complex (Aplin, et al. 2011). The spread of agriculture
113 and subsequent trade spurred regional and global range expansion of black rats. Genetic evidence
114 indicates that the global distribution of *R. rattus* Lineage I began with an expansion from the
115 Indian subcontinent into western Asia, followed by separate expansions into Europe and Africa
116 (Tollenaere, et al. 2010; Aplin, et al. 2011). The presence of derived haplotypes also indicates
117 that *R. rattus* Lineage I colonized the Americas, Oceania, and Africa from Europe (Aplin, et al.
118 2011; Bastos, et al. 2011).

119
120 Elucidating global brown rat phylogeographic patterns has several important implications. First,
121 the spread of brown rats may illuminate patterns of human connectivity via trade, or unexpected
122 movement patterns as observed in other commensal rodents (Searle, et al. 2009). Second, rats are
123 hosts to many zoonotic diseases (e.g., *Leptospira interrogans*, Seoul hantavirus, etc.);
124 understanding the distribution of genomic backgrounds may provide insight into differential
125 disease susceptibilities. Additionally, an understanding of contemporary population structure in
126 rats may elucidate source and sink areas for disease transmission. Third, brown rat eradication
127 programs occur in urban areas to decrease disease transmission and on islands where rats prey
128 upon native fauna. A comprehensive understanding of global population structure will allow for
129 better design of eradication efforts, particularly for understanding how to limit new invasions.
130 Thus, our aim was to test biological hypotheses developed from an understanding of the

131 historical narrative of spread using phylogeographic inference. We estimated the number of
132 distinct clusters around the world, the genomic contribution of these clusters within invaded
133 areas, and whether genetic drift and/or post-colonization admixture elicits evolutionary
134 divergence from source populations.

135

136 **RESULTS and DISCUSSION**

137 *Evolutionary Clustering*

138 *Nuclear Genome-* Our analyses of 314 rats using 32,127 single nucleotide polymorphisms
139 (SNPs) from ddRAD-Seq identified multiple hierarchical levels of evolutionary clustering (K).
140 Principal component analysis (PCA) distinguished two clusters along the first principal
141 component (PC), an Asian cluster that extended to western North America, and a non-Asian
142 cluster found in Europe, Africa, the Americas, and New Zealand (Fig. 1). Higher dimension PCA
143 axes distinguished subclusters (Fig. S2), then individual sampling sites; in total 58 axes of
144 variation were significant using Tracy-Widom statistics (20 and 37 axes were significant for
145 PCAs with only Asian or non-Asian samples respectively). Using the model-based clustering
146 program ADMIXTURE, the Asian and non-Asian clusters divided into five and eight
147 subclusters, respectively (Fig. 2, 3, S3-S5). Higher numbers of clusters (K=18, 20, and 26) were
148 also supported by ADMIXTURE (Fig. S3A, S4), distinguishing ever finer spatial scales (from
149 subcontinents to cities).

150

151 The subclusters in the Asian cluster reflect underlying geography and hierarchical differentiation
152 (Fig. S3B). The predominant four clusters reflected differentiation between: China, Southeast
153 (SE) Asia, the Aleutian Archipelago, and Western North America (Fig. S6, S7). Within the SE
154 Asia cluster, further subdivision was observed for the Philippines and Thailand (Fig. 2, S7).
155 Within the Aleutian Archipelago cluster, samples from the city of Sitka (in the Alexander
156 Archipelago) formed a subcluster. Rats from the Russian city of Sakhalinskaya Oblast and four
157 rats aboard the Bangun Perkasa ship each formed a subcluster (Fig. S7). The Bangun Perkasa
158 was a nationless vessel seized in the Pacific Ocean by the US government in 2012 for illegal
159 fishing. Our analyses identified that the rats aboard were of SE Asian origin and likely
160 represented a city in that region, probably one bordering the South China Sea, at which the ship
161 originated or docked.

162

163 We detected greater hierarchical differentiation in the non-Asian cluster (Fig. S3C). At K=3 we
164 observed divergence between the Western Europe (W Euro) and Northern Europe (N Euro)
165 clusters (Fig. S9). The W Euro cluster contained rats from Europe (Great Britain, France,
166 Austria, and Hungary), Central and South America (Argentina, Brazil, Chile, Galapagos Islands,
167 Honduras, Guatemala, Panama), the Caribbean (Barbados, Saint Lucia), North America (eastern,
168 central, and western USA), New Zealand, and Africa (Senegal and Mali); and the N Euro cluster
169 included Norway, Sweden, Finland, Germany, and the Netherlands (Fig. 2, S4, S8, S9). Within
170 these broad geographic regions, many subclusters were identified by ADMIXTURE that likely
171 resulted from either intense founder effects, isolation resulting in genetic drift, the inclusion of
172 second and third order relatives in the dataset, or a combination of these factors. In the global
173 analysis, four clusters were nested within W Euro (the island of Haida Gwaii, Canada;
174 Vancouver, Canada; Kano, Nigeria; and Sonoma County in the western USA) and two within N
175 Euro (Bergen, Norway; Malmo, Sweden). We identified additional well-supported subclusters
176 within the non-Asian cluster at K=12, 15, and 17 that represented individual cities (Fig. S9).

177

178 Our analysis using FINESTRUCTURE identified 101 clusters (Fig. 3). Of the 39 cities where
179 more than one individual was sampled, 19 cities supported multiple clusters indicating genetic
180 differentiation within cities. As GPS coordinates were not collected, we cannot hypothesize if
181 these clusters represent distinct populations or were artefacts of sampling relatives, despite
182 removal of individuals with relatedness coefficients greater than 0.20, although the
183 FINESTRUCTURE algorithm should be robust to relatedness when identifying clusters. The
184 Asian and N Euro sampling sites individually had higher coancestry coefficients between
185 locations (Fig. 3) which supported the hierarchical clustering observed using ADMIXTURE.

186

187 *Mitochondrial Genome*- We identified 10 clades within a network-based analysis of 103
188 mitochondrial haplotypes (Fig. 4, Tables S5, S6). Many of the clades had spatial structure
189 concordant with the nuclear genome results (Fig. 2A). We observed clade 1 in China, Russia,
190 and western North America. Additionally, clades 6 and 9 contained a single haplotype only
191 observed in China. We interpret the diversity of clades within northern China as representative of
192 geographic structure in the ancestral range prior to movement of rats by humans (Fig. 4, Table

193 S6). In SE Asia we observed clades 2 (aboard the Bangun Perkasa), 3 (Philippines), and 5
194 (Cambodia, Thailand, and Vietnam). Clade 4 was found in western North America. European
195 samples comprised three divergent clades (3, 8, and 10). Clade 8 was observed across Europe,
196 western North America, and South America; this clade shared ancestry with clade 7 which was
197 observed in Russia and Thailand (Fig. 4).

198

199 *Range Expansion*

200 We thinned our dataset to the sampling site with the largest sample size within each of the 13
201 clusters supported by ADMIXTURE and analyzed the data using TREEMIX (Fig. S10). We
202 observed divergence within Asia first, followed by the two independent expansions into western
203 North America. Drift along the backbone of the non-Asian cluster was limited, indicating rapid
204 expansion of rats into Africa, Europe, and the Americas (Fig. S10). Both the population tree
205 topology and PCA (Figs. 1, S2, S10) indicated that range expansion occurred in three directions,
206 where one southward and two eastward expansions comprised Asian ancestry, and the westward
207 expansion produced the non-Asian cluster.

208

209 *Ancestral Range-* In eastern China, the nuclear genome assigned strongly to a single cluster
210 while mitochondrial diversity encompassed two divergent clades, where samples from western
211 China assigned to both the Chinese and SE Asian clusters and represented a third mitochondrial
212 clade. This result suggests substructure within the ancestral range, although the samples from
213 northeastern China may not be representative of the ancestral range but instead of an isolated,
214 divergent population that has retained high genetic diversity (Tables S4, S6).

215

216 *Southern Expansion into SE Asia-* A southward range expansion into SE Asia was supported by
217 the population tree topology, higher heterozygosity, low nuclear F_{ST} with China, and elevated
218 coancestry coefficients between populations in SE Asia, China, and Russia (Fig. 3, Tables S3,
219 S4). Given evidence for an early southward expansion (Fig. S10), we hypothesize that the
220 founding of SE Asia was accompanied by a weak bottleneck resulting in relatively low loss of
221 genetic diversity. However, following founding regional diversification occurred as we observed
222 substructure in both the nuclear and mitochondrial genomes (Fig. 2, 4, S7).

223

224 *Two Independent Eastward Expansions* - We observed population divergence along the first
225 eastward expansion from eastern Russia into the Aleutian Archipelago based on PCA (Fig. S6).
226 Both the population tree topology and PCA indicate that a second eastward expansion progressed
227 from Asia to western North America (Fig. S6, S10). While the Western North America cluster
228 was observed in both northern and southern Pacific coast localities (Fig. S5A), we cannot
229 extrapolate that this cluster represents the entirety of the coastline. Specifically, Sitka, Ketchikan,
230 Vancouver, and the Bay Area are all located between the Alaskan cities and San Diego County
231 that comprise the Western North America cluster. Further, the timing of these expansions is an
232 open question. While the population tree indicated divergence of these two expansions prior to
233 divergence of the non-Asian cluster, the historical record attributes brown rats in the Aleutian
234 Archipelago to Russian fur traders in the 1780s (Black 1983), which is not consistent with rats
235 entering Europe in the 1500s (Armitage 1993). Thus, evidence of early divergence may be a
236 consequence of unsampled Asian populations sharing ancestry with the Aleutian Archipelago
237 and Western North America clusters.

238
239 *Westward Range Expansion into Europe*- The low drift along the backbone of the population tree
240 for the non-Asian cluster is indicative of rapid westward expansion (Fig. S10). Limited
241 inferences could be drawn about western Asia and the Middle East because of sampling
242 constraints, but we hypothesize that the region was colonized by the range expansion of the non-
243 Asian cluster. We observed three mitochondrial clades in Europe, where clade 3 shared ancestry
244 with SE Asia and clade 8 shared ancestry with eastern Russia, while clade 10 is a European
245 derived clade (Fig. 3, Table S6). Thus, Europe may have been independently colonized three
246 times, although the routes remain an open question. We hypothesize that clade 10 arrived
247 overland around the Mediterranean Sea, similar to black rats (Aplin, et al. 2011). We hypothesize
248 that following the independent colonizations, the genetic backgrounds admixed prior to
249 divergence between the N Euro and W Euro clusters given the low nuclear F_{ST} (Table S4).

250
251 Notably, we detected genetic differentiation of Bergen, Norway and Malmo, Sweden within the
252 N Euro cluster (Fig. 2). This pattern suggests drift following either a strong founder effect or
253 population isolation and limited gene flow. Isolation is likely driving the pattern observed in

254 Bergen, which is separated from eastern Norway by mountains that are thought to limit
255 movement of commensal rodents (Jones, et al. 2010).

256

257 *Range Expansion of Rats by Europeans*

258 We detected a fifth range expansion that can be attributed to transport by western European
259 imperial powers (1600s-1800s) to former colonial territories (Fig. 2, 3, S4, S9). For example, we
260 observed high proportions of W Euro ancestry in samples from the North and South Islands of
261 New Zealand, which is consistent with the introduction of brown rats by British colonists, as has
262 also been inferred for black rats (Aplin, et al. 2011) and domestic cats in Australia (Spencer, et
263 al. 2016). We observed admixture on both islands (Fig. 3) although nuclear ancestry proportions
264 differed between the islands with higher proportions of N Euro and Vancouver ancestry on the
265 North Island. The South Island had higher SE Asia and Western North American ancestry (Fig.
266 2, 3, S4); these ancestry components may be attributed to the seal skin trade with southern China
267 by sealers from the USA (King 2016).

268

269 The samples from Nigeria and Mali formed a sister clade in FINESTRUCTURE, which likely
270 reflects a shared history as French colonies, although Senegal fell outside of the clade (Fig. 3).
271 Mali had elevated W Euro ancestry compared to Nigeria which may be a consequence of
272 multiple introductions from European sources. South American countries exhibited a
273 paraphyletic FINESTRUCTURE topology that is suggestive of colonization from multiple
274 locations. This result was also supported by the presence of all three mitochondrial clades found
275 in Europe (Fig. 4A). Further sampling from Portugal and Spain would better resolve the origins
276 of Brazilian populations and clarify relationships of former colonies elsewhere in the world.

277

278 The complex distribution of clusters in North America is suggestive of a dynamic colonization
279 history, including independent introductions on both the Atlantic and Pacific coasts (Fig. 2). We
280 detected mtDNA haplotypes of European ancestry in the eastern and central USA, whereas the
281 Pacific seaboard harbors high mtDNA haplotype diversity from European and Asian clades (Fig.
282 4). These results are consistent with prior observations of four high-frequency mtDNA
283 haplotypes across Alaska and the continental USA, of which three were observed in east Asia
284 and one in Europe (Lack, et al. 2013). Along the Pacific coast, cities with both Asian and non-

285 Asian nuclear ancestry were observed (Fig. 2), which parallels the pattern observed in black rats
286 (Aplin, et al. 2011). Given the bicoastal introductions, it is unsurprising to observe admixture in
287 North American cities such as the San Francisco Bay Area and Albuquerque, where each has
288 elevated coancestry coefficients with Asian and non-Asian clusters (Fig. 3). We also observed
289 limited eastward dispersal of Asian genotypes, although other work has found evidence of
290 greater inland penetration (Lack, et al. 2013).

291
292 Rats from Haida Gwaii off the coast of British Columbia, Canada, were consistently recovered as
293 a separate cluster in ADMIXTURE, and had high coancestry coefficients and F_{ST} with other
294 populations (Fig. 3, Table S4), indicating substantial genetic drift following colonization. Rats
295 were introduced to Haida Gwaii in the late 1700s via Spanish and/or British mariners, and have
296 been subject to recent, intensive eradication efforts that may have heightened genetic drift
297 (Hobson, et al. 1999).

298 299 *Intra-urban Population Structure of Brown Rats*

300 Brown rats exhibit population structure over a remarkably fine-grained spatial scale (Fig. 3);
301 specifically, rat population structure exists at the scale of both cities and neighborhoods. We
302 found evidence of heterogeneity among cities as some appear to support one population while
303 others support multiple populations. For example, we detected a single population across
304 multiple neighborhoods in Manhattan (NYC, USA), whereas four genetic clusters (Fig. 3) were
305 observed in a neighborhood in Salvador, Brazil, a result that confirmed previous microsatellite
306 based analyses (Kajdacsí, et al. 2013). Although denser sampling will be needed to confirm
307 whether these groups represent distinct populations or reflect oversampling of intra-city pockets
308 of highly related individuals, intra-city clustering likely represents substructure considering the
309 global design of our SNP dataset. Observations of highly variable intra-city structure suggest the
310 following three scenarios: first, effective population size rapidly increases after invasion,
311 possibly driven by high urban resource levels, and thus genetic drift may have a relatively weak
312 effect on population differentiation. Second, new immigrants that arrive after initial invasion and
313 establishment of rats in a city may be limited in their capacity to either establish new colonies or
314 join existing colonies (Calhoun 1962), thereby limiting ongoing gene flow from other areas due
315 to competitive exclusion (Waters 2011). Gene flow into colonies may also be sex-biased as

316 females were recruited more readily than males in a two-year behavioral study of brown rats
317 (Calhoun 1962). We did observe gene flow in our dataset, including an individual matching
318 Coastal Alaska into the Bay Area and an individual with high Sonoma Valley ancestry in
319 Thailand (Fig. 2B), thus migration due to contemporary human-assisted movement is possible
320 and ongoing. However, given increasing connectivity due to trade and continual movement of
321 invasive species (Banks, et al. 2015), we expected greater variability in ancestry proportions
322 within cities than observed (Fig. S4). Third, cityscapes vary in their connectivity where some
323 cities contain strong physical and/or environmental barriers facilitating differentiation and others
324 do not. Identifying commonalities and differences among cityscapes with one or multiple rat
325 populations should be a goal for understanding how rats interact with their environment,
326 particularly in relation to the effect of landscape connectivity for pest and disease control efforts.

327

328 *Significance*

329 *Understanding the Spread of Zoonotic Pathogens-* Understanding the global population structure
330 of brown rats offers novel perspectives on the forces driving the spread of zoonotic disease. Our
331 inference that competitive exclusion may limit entry into established populations helps explain
332 why zoonotic pathogens do not always exhibit the same spatial distribution as rat hosts as well as
333 the patchy distribution of presumably ubiquitous pathogens within and between cities
334 (Himsworth, et al. 2013). While within-colony transmission of disease and natal dispersal
335 between colonies are important factors related to the prevalence of zoonotic disease, our results
336 also suggest that contemporary human-aided transport of infected rats does not contribute to the
337 global spread of pathogens, as we would expect higher variability of ancestry proportions within
338 cities if rats were successfully migrating between cities. Additionally, our results indicate that
339 rats with different genomic backgrounds may have variable susceptibilities to pathogens, though
340 differential susceptibility likely depends on concordance between the geographic origins of
341 pathogens and rats. While this idea needs pathogen specific testing, it could have substantial
342 implications for global disease transmission.

343

344 *Rat Eradication Programs for Species Conservation-* Eradication of invasive *Rattus* species on
345 islands and in ecosystems with high biodiversity is a priority for conservation of at-risk species,
346 as rats outcompete or kill native fauna. It remains challenging to gauge the success of eradication

347 programs, because it is difficult to distinguish between post-intervention survival and
348 reproduction as opposed to recolonization by new immigrants (Piertney, et al. 2016).
349 Understanding fine-scale population genetic structure using dense nuclear marker sets (Robins,
350 et al. 2016), as in this study, would allow managers to more clearly assess outcomes and next
351 steps following an eradication campaign. For example, genomic analyses could illustrate that an
352 area has been recolonized by immigration from specific source populations, thereby allowing
353 managers to shift efforts towards biosecurity to reduce the likelihood of establishment by
354 limiting the influx of potential immigrants.

355

356 **MATERIALS and METHODS**

357 We obtained rat tissue samples from field-trapped specimens, museum or institute collections,
358 and wildlife markets (Tables S1, S2). As GPS coordinates for individuals were not always
359 available, the sampling location was recorded as either the city, nearest town, or island where
360 rats were collected.

361

362 *DNA Extraction, RAD sequencing, and SNP calling*

363 We extracted DNA following the manufacturer's protocols using Qiagen DNeasy kits (Valencia,
364 CA). We prepared double digest restriction-site associated DNA sequencing (ddRAD-Seq)
365 libraries with 500-1000ng of genomic DNA from each sample and one negative control made up
366 of water. Briefly, samples were digested with SphI and MluCI before ligation of unique barcoded
367 adapters. We pooled 48 barcoded samples each in 10 libraries at equimolar concentrations. We
368 then selected fragments from 340-412 bp (target = 376 bp) using a Pippin Prep (Sage Science,
369 Beverly, MA). The size-selected pools were PCR-amplified for 10-12 cycles using Phusion PCR
370 reagents (New England Biolabs, Ipswich, MA) and primers that added an Illumina multiplexing
371 read index. Final libraries were checked for concentration and fragment size on a BioAnalyzer
372 (Agilent Technologies, Santa Clara, CA), then sequenced (2 x 125bp paired-end) at the New
373 York Genome Center across five lanes of an Illumina HiSeq 2500.

374

375 We demultiplexed the raw reads using the process_radtags script in STACKS v1.35 (Catchen, et
376 al. 2013), then aligned reads for each individual to the *Rattus norvegicus* reference genome
377 (Rnor_6.0) (Gibbs, et al. 2004) using Bowtie v2.2.6 (Langmead and Salzberg 2012) with default

378 parameters. To assess the number of mismatches allowed between stacks and the minimum depth
379 of coverage for each stack when building RADtags (-n and -m flags respectively) in STACKS,
380 we processed two samples under a number of scenarios and compared the number of RADtags
381 that formed as de novo loci versus those that mapped to the reference *R. norvegicus* genome. We
382 first assessed the M parameter by holding m constant at three while varying M between two and
383 five in the ustacks program. We observed a decrease in the undermerged RADs with increasing
384 values of M; we selected M = 4 for both the final RAD processing and as the constant level when
385 we allowed m to vary between two and five. We selected m = 3 to balance between removing
386 real loci and stacks that erroneously mapped to the reference genome. In the cstacks program we
387 assessed the number of allowed mismatches between tags (n) from zero to two. We observed
388 little difference for this parameter between our test values and decided to use n = 2 as a
389 conservative measure.

390

391 We initially built the STACKS catalog with all of the reference-aligned samples (n = 447) using
392 the ref_map pipeline. Following processing, we filtered for the following: biallelic SNPs, a
393 minor allele frequency (MAF) greater than or equal to 0.05, SNPs genotyped in 80% of samples,
394 and only one SNP per RADtag (STACKS flag --write_single_snp); additionally, SNPs that
395 mapped to either the Y chromosome or mitochondrial genome were removed. This dataset had
396 37,730 SNPs. Following sample collection and genotyping, we were informed that *R. rattus*
397 samples had been collected in Mali; we capitalized on this by confirming the species
398 identification for each sample using principal components analysis (PCA) in EIGENSOFT
399 v5.0.2 (Patterson, et al. 2006; Price, et al. 2006), and ADMIXTURE v1.23 (Alexander, et al.
400 2009) for two clusters. We identified 33 *R. rattus* and 414 *R. norvegicus* samples (Fig. S1).

401

402 We reran ref_map using only the confirmed *R. norvegicus* samples, and filtered similarly as
403 described above plus an additional filter to remove individuals with greater than 60% missing
404 data. To add genotypes from 11 of the *R. norvegicus* samples collected in Harbin, China
405 (European Nucleotide Archive ERP001276) (Deinum, et al. 2015), we mapped reads to the
406 Rnor_6.0 genome using SAMTOOLS v1.2 (Li, et al. 2009) then extracted the SNP dataset using
407 mpileup with a position list. We removed related individuals within, but not between, sampling
408 sites by assessing relatedness in KING v1.4 (Manichaikul, et al. 2010). For each pair of

409 individuals with relatedness estimators greater than 0.2, one individual was removed from the
410 analysis ($n = 22$). Subsequently, we randomly thinned 14 samples from Vancouver, Canada as
411 preliminary analyses indicated oversampling. Thus the final nuclear *R. norvegicus* dataset
412 contained 32,127 SNPs genotyped in 314 individuals (Table S1).

413
414 From the initial processing in STACKS, we extracted the SNPs that mapped to the mitochondrial
415 genome to produce a second dataset with 115 SNPs (see Table S5 for base pair positions within
416 the *R. norvegicus* reference mitochondrial genome, GenBank accession AY172581.1). We
417 extracted the same positions from the mitochondrial genomes of samples from Harbin, China.
418 We allowed up to 35% missing data per individual and identified 103 haplotypes using
419 COLLAPSE v1.2 (Posada 2004) in 144 individuals. We built a haplotype network using
420 SPLITSTREE v4.13.1 (Huson and Bryant 2006) and identified the haplotypes grouped into 10
421 clades (Table S6).

422 423 *Population Genomic Analyses*

424 To describe population structure, we ran ADMIXTURE (Alexander, et al. 2009) at each cluster
425 from 1 to 40. Given known effects of sampling bias on clustering analyses, we repeated this
426 analysis with a subset of the data where four or five samples from each city were randomly
427 selected ($n = 158$). The results supported $K=14$ clusters which supported the analysis of our full
428 dataset. We also subdivided the full dataset into the Asian and non-Asian clusters and reran
429 ADMIXTURE at each cluster from 1 to 25. We used the CV error values to identify the best-
430 supported clustering patterns across the range. Using the same datasets (full, Asian, and non-
431 Asian), we ran PCA in EIGENSOFT (Patterson, et al. 2012) and identified significant PCs using
432 Tracy-Widom statistics.

433
434 We also estimated evolutionary clusters using FINESTRUCTURE v2.0.7 (Lawson, et al. 2012)
435 which elucidates the finest grained clusters by accounting for linkage disequilibrium and allows
436 detailed admixture inference based upon the pairwise coancestry coefficients. We limited this
437 analysis to the 20 autosomes (31,489 SNPs), removing SNPs on unassembled scaffolds in the
438 dataset. Data for each chromosome were phased and imputed using fastPHASE v1.2 (Scheet and
439 Stephens 2006). Initial analyses using the linked model indicated our data were effectively

440 unlinked (c-factor 0.0104); therefore, we ran the unlinked model. We used default settings except
441 for the following parameters: 25% of the data were used for initial EM estimation; 750,000
442 iterations of the MCMC were run (375,000 of which were burnin) with 1,000 samples retained,
443 20,000 tree comparisons, and 500,000 steps of the tree maximization were run. We viewed
444 MCMC trace files to confirm stability of all parameters.

445

446 To understand patterns of population divergence, we ran TREEMIX v1.12 (Pickrell and
447 Pritchard 2012). As the *R. rattus* data (see Supplemental Methods) were mapped to the *R.*
448 *norvegicus* genome, we extracted SNPs at the same genomic positions for 31 black rats (we
449 removed two samples showing admixture; Fig. S1) with SAMTOOLS (Li, et al. 2009) mpileup
450 function using a position list. We selected the sampling location with the largest sample size
451 from each of the well supported clusters at K=13 (Fig. 2, S4), plus the *R. rattus* samples for the
452 outgroup (which were not subdivided due to lack of population structure, Fig. S11). We added
453 migration edges to the population tree sequentially by fixing the population tree to the tree with
454 n-1 migration edges, where blocks of 1,000 SNPs and the sample size correction were enabled.
455 We assessed both the proportion of variance (Fig. S12A) and the residuals of the population tree
456 (Fig. S12B) and chose the model with three migration edges. We decided to thin the sampling
457 areas due to uneven sampling between the broad Asian and non-Asian clusters; both factors
458 should affect the variance in the model, thus we presented a potentially underfit versus overfit
459 model. We ran f_3 tests within TREEMIX and observed no significant relationships, likely due to
460 highly complex admixture patterns (Patterson, et al. 2012).

461

462 For the nuclear dataset, we calculated expected heterozygosity (H_E) and F_{IS} within each of the 13
463 clusters using ARLEQUIN v3.5.1.3 (Excoffier and Lischer 2010), and pairwise F_{ST} using
464 VCFTOOLS v0.1.13 and the Weir and Cockerham estimator (Weir and Cockerham 1984;
465 Danecek, et al. 2011). For the mitochondrial dataset, we calculated pairwise F_{ST} between the
466 clusters identified in the nuclear dataset in ARLEQUIN.

467

468 **ACKNOWLEDGEMENTS**

469 This work was funded by National Science Foundation grants DEB 1457523 and DBI 1531639,
470 and a Fordham University faculty research grant, to JM-S. We thank Kaitlin Abrams and Ian

471 Hays for assisting with lab work. We thank Annette Backhans, Francois Catzefflis, Gauthier
472 Dobigny, Carol Esson, Tim Giles, Gregory Glass, Sabra Klein, Mare Löhmus, Patrick McClure,
473 Frank van de Goot, Jordan Reed and his Mongrel Hoard, Richard Reynolds and the Ryders Alley
474 Trencher-fed Society (R.A.T.S), Thomas Persson Vinnersten and colleagues at Anticimex, and
475 partners of the Network Rodent-Borne Pathogens for collecting and providing rat samples. The
476 mammal collections at the University of Alaska Museum of the North, Angelo State University,
477 Berkeley Museum of Comparative Zoology, the Burke Museum at University of Washington, the
478 Museum of Southwestern Biology, and the Museum of Texas Tech University also graciously
479 provided tissue samples.

480 **REFERENCES**

481

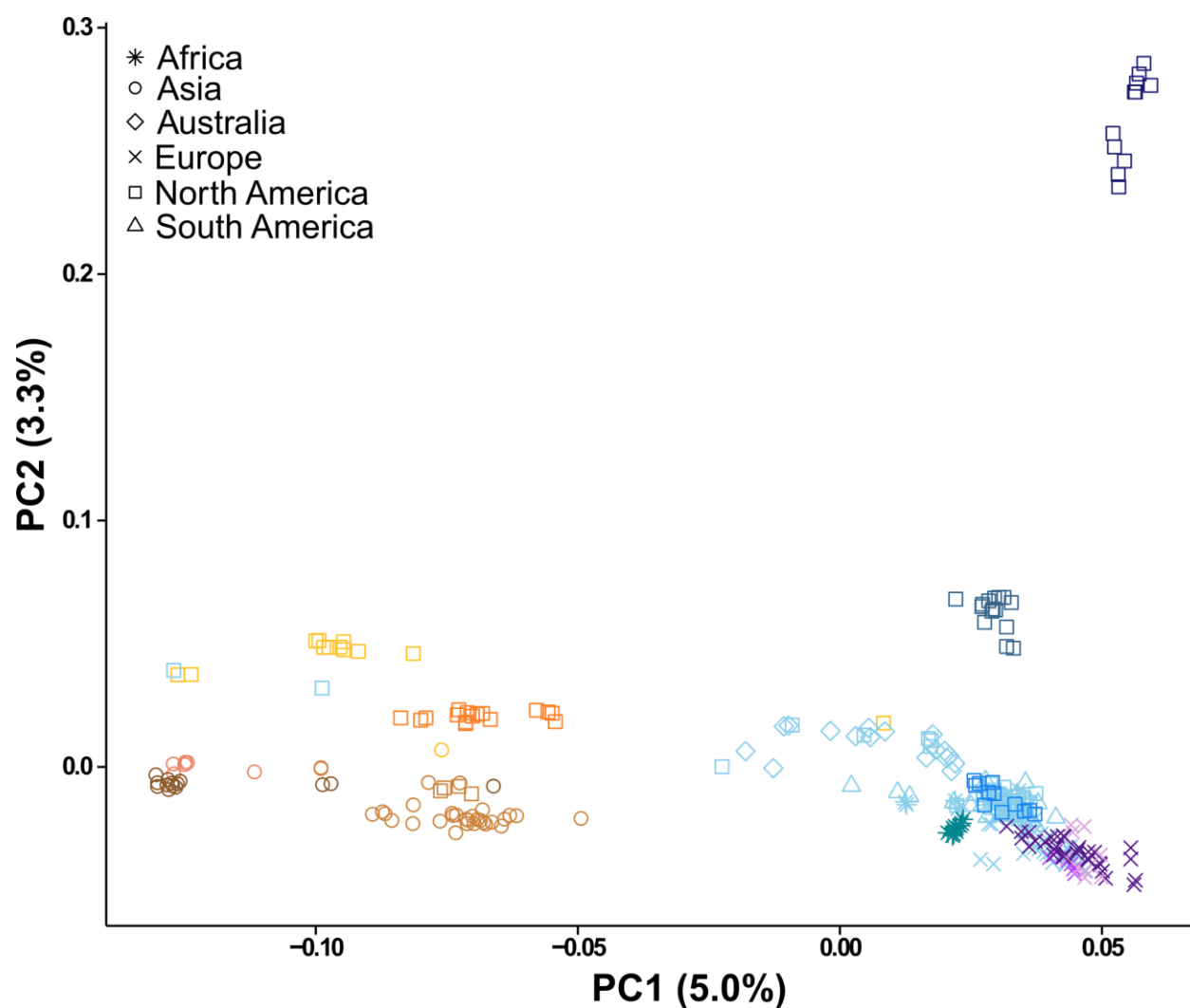
- 482 Alexander DH, Novembre J, Lange K. 2009. Fast model-based estimation of ancestry in
483 unrelated individuals. *Genome Research* 19:1655-1664.
- 484 Aplin KP, Suzuki H, Chinen AA, Chesser RT, ten Have J, Donnellan SC, Austin J, Frost A,
485 Gonzalez JP, Herbreteau V, et al. 2011. Multiple geographic origins of commensalism and
486 complex dispersal history of black rats. *Plos One* 6:e26357.
- 487 Armitage P. 1993. Commensal rats in the New World, 1492-1992. *Biologist* 40:174-178.
- 488 Banks NC, Paine DR, Bayliss KL, Hodda M. 2015. The role of global trade and transport
489 network topology in the human-mediated dispersal of alien species. *Ecology Letters* 18:188-199.
- 490 Bastos AD, Nair D, Taylor PJ, Brettschneider H, Kirsten F, Mostert E, von Maltitz E, Lamb JM,
491 van Hooft P, Belmain SR, et al. 2011. Genetic monitoring detects an overlooked cryptic species
492 and reveals the diversity and distribution of three invasive *Rattus* congeners in South Africa.
493 *Bmc Genetics* 12:26.
- 494 Black L editor. Proceedings of the Alaska Maritime Archaeology Workshop, May 17-19, 1983.
495 1983 May 17-19, 1983: Sitka, AK.
- 496 Calhoun JB. 1962. The Ecology and Sociology of the Norway Rat. In: US Department of Health
497 E, and Welfare, editor. Washington DC: Public Health Service. p. 288.
- 498 Catchen J, Hohenlohe PA, Bassham S, Amores A, Cresko WA. 2013. STACKS: an analysis tool
499 set for population genomics. *Molecular Ecology* 22:3124-3140.
- 500 Cucchi T, Vigne J-D, Auffray J-C. 2005. First occurrence of the house mouse (*Mus musculus*
501 *domesticus* Schwarz & Schwarz, 1943) in the Western Mediterranean: a zooarchaeological
502 revision of subfossil occurrences. *Biological Journal of the Linnean Society* 84:429-445.
- 503 Danecek P, Auton A, Abecasis G, Albers CA, Banks E, DePristo MA, Handsaker RE, Lunter G,
504 Marth GT, Sherry ST, et al. 2011. The variant call format and VCFtools. *Bioinformatics*
505 27:2156-2158.
- 506 Deinum EE, Halligan DL, Ness RW, Zhang Y-H, Cong L, Zhang J-X, Keightley PD. 2015.
507 Recent evolution in *Rattus norvegicus* is shaped by declining effective population size.
508 *Molecular Biology and Evolution* 32:2547-2558.
- 509 Excoffier L, Lischer HEL. 2010. Arlequin suite ver 3.5: a new series of programs to perform
510 population genetics analyses under Linux and Windows. *Molecular Ecology Resources* 10:564-
511 567.
- 512 Gabriel SI, Mathias ML, Searle JB. 2015. Of mice and the ‘Age of Discovery’: the complex
513 history of colonization of the Azorean archipelago by the house mouse (*Mus musculus*) as
514 revealed by mitochondrial DNA variation. *Journal of Evolutionary Biology* 28:130-145.
- 515 Gibbs RA, Weinstock GM, Metzker ML, Muzny DM, Sodergren EJ, Scherer S, Scott G, Steffen
516 D, Worley KC, Burch PE, et al. 2004. Genome sequence of the Brown Norway rat yields
517 insights into mammalian evolution. *Nature* 428:493-521.

- 518 Harper GA, Bunbury N. 2015. Invasive rats on tropical islands: Their population biology and
519 impacts on native species. *Global Ecology and Conservation* 3:607-627.
- 520 Himsworth CG, Parsons KL, Jardine C, Patrick DM. 2013. Rats, cities, people, and pathogens: a
521 systematic review and narrative synthesis of literature regarding the ecology of rat-associated
522 zoonoses in urban centers. *Vector Borne Zoonotic Dis* 13:349-359.
- 523 Hobson KA, Drever MC, Kaiser GW. 1999. Norway Rats as Predators of Burrow-Nesting
524 Seabirds: Insights from Stable Isotope Analyses. *The Journal of Wildlife Management* 63:14-25.
- 525 Hulme-Beaman A, Dobney K, Cucchi T, Searle JB. In Press. An ecological and evolutionary
526 framework for commensalism in anthropogenic environments. *Trends in Ecology & Evolution*.
- 527 Huson DH, Bryant D. 2006. Application of phylogenetic networks in evolutionary studies.
528 *Molecular Biology and Evolution* 23:254-267.
- 529 Jing M, Yu H-T, Bi X, Lai Y-C, Jiang W, Huang L. 2014. Phylogeography of Chinese house
530 mice (*Mus musculus musculus/castaneus*): Distribution, routes of colonization and geographic
531 regions of hybridization. *Molecular Ecology* 23:4387-4405.
- 532 Jones EP, Eager HM, Gabriel SI, Jóhannesdóttir F, Searle JB. 2013. Genetic tracking of mice
533 and other bioproxies to infer human history. *Trends in Genetics* 29:298-308.
- 534 Jones EP, Van Der Kooij J, Solheim R, Searle JB. 2010. Norwegian house mice (*Mus musculus*
535 *musculus/domesticus*): distributions, routes of colonization and patterns of hybridization.
536 *Molecular Ecology* 19:5252-5264.
- 537 Kajdacsí B, Costa F, Hyseni C, Porter F, Brown J, Rodrigues G, Farias H, Reis MG, Childs JE,
538 Ko AI, et al. 2013. Urban population genetics of slum-dwelling rats (*Rattus norvegicus*) in
539 Salvador, Brazil. *Molecular Ecology* 22:5056-5070.
- 540 King CM. (King2016 co-authors). 2016. How genetics, history and geography limit potential
541 explanations of invasions by house mice *Mus musculus* in New Zealand. *Biological Invasions*
542 18:1533-1550.
- 543 Lack J, Hamilton M, Braun J, Mares M, Van Den Bussche R. 2013. Comparative
544 phylogeography of invasive *Rattus rattus* and *Rattus norvegicus* in the U.S. reveals distinct
545 colonization histories and dispersal. *Biological Invasions* 15:1067-1087.
- 546 Lack JB, Greene DU, Conroy CJ, Hamilton MJ, Braun JK, Mares MA, Van Den Bussche RA.
547 2012. Invasion facilitates hybridization with introgression in the *Rattus rattus* species complex.
548 *Molecular Ecology* 21:3545-3561.
- 549 Langmead B, Salzberg SL. 2012. Fast gapped-read alignment with Bowtie 2. *Nat Meth* 9:357-
550 359.
- 551 Lawson DJ, Hellenthal G, Myers S, Falush D. 2012. Inference of population structure using
552 dense haplotype data. *Plos Genetics* 8:e1002453.
- 553 Li H, Handsaker B, Wysoker A, Fennell T, Ruan J, Homer N, Marth G, Abecasis G, Durbin R.
554 2009. The Sequence Alignment/Map format and SAMtools. *Bioinformatics* 25:2078-2079.
- 555 Long JL. 2003. *Introduced Mammals of the World: Their History, Distribution and Influence*.
556 Collingwood, Australia: CSIRO Publishing.

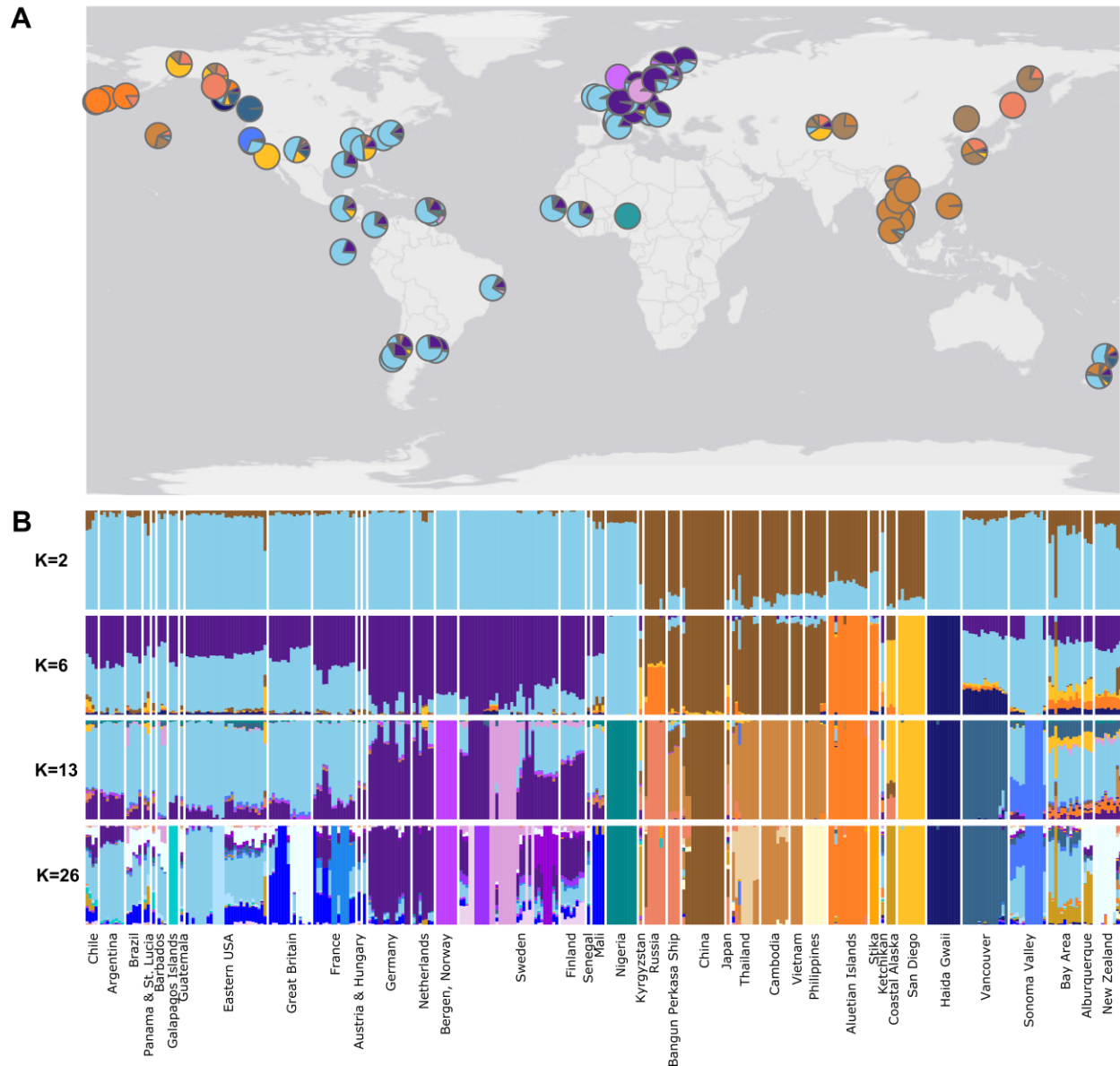
- 557 Manichaikul A, Mychaleckyj JC, Rich SS, Daly K, Sale M, Chen WM. 2010. Robust
558 relationship inference in genome-wide association studies. *Bioinformatics* 26:2867-2873.
- 559 Matisoo-Smith E, Robins JH. 2004. Origins and dispersals of Pacific peoples: Evidence from
560 mtDNA phylogenies of the Pacific rat. *Proceedings of the National Academy of Sciences of the*
561 *United States of America* 101:9167-9172.
- 562 Patterson N, Moorjani P, Luo Y, Mallick S, Rohland N, Zhan Y, Genschoreck T, Webster T,
563 Reich D. 2012. Ancient admixture in human history. *Genetics* 192:1065-1093.
- 564 Patterson N, Price AL, Reich D. 2006. Population structure and eigenanalysis. *Plos Genetics*
565 2:e190.
- 566 Pickrell JK, Pritchard JK. 2012. Inference of population splits and mixtures from genome-wide
567 allele frequency data. *PLoS Genet* 8:e1002967.
- 568 Piertney SB, Black A, Watt L, Christie D, Poncet S, Collins MA. 2016. Resolving patterns of
569 population genetic and phylogeographic structure to inform control and eradication initiatives for
570 brown rats *Rattus norvegicus* on South Georgia. *Journal of Applied Ecology* 53:332-339.
- 571 Pimentel D, Lach L, Zuniga R, Morrison D. 2000. Environmental and Economic Costs of
572 Nonindigenous Species in the United States. *Bioscience* 50:53-65.
- 573 Posada D. 2004. *Collapse v1.2*.
- 574 Prager EM, Orrego C, Sage RD. 1998. Genetic variation and phylogeography of central Asian
575 and other house mice, including a major new mitochondrial lineage in Yemen. *Genetics*
576 150:835-861.
- 577 Price AL, Patterson NJ, Plenge RM, Weinblatt ME, Shadick NA, Reich D. 2006. Principal
578 components analysis corrects for stratification in genome-wide association studies. *Nature*
579 *Genetics* 38:904-909.
- 580 Robins JH, Miller SD, Russell JC, Harper GA, Fewster RM. 2016. Where did the rats of Big
581 South Cape Island come from? *New Zealand Journal of Ecology* 40:229-234.
- 582 Scheet P, Stephens M. 2006. A fast and flexible statistical model for large-scale population
583 genotype data: Applications to inferring missing genotypes and haplotypic phase. *American*
584 *Journal of Human Genetics* 78:629-644.
- 585 Searle JB, Jones CS, Gündüz İ, Scascitelli M, Jones EP, Herman JS, Rambau RV, Noble LR,
586 Berry RJ, Giménez MD, et al. 2009. Of mice and (Viking?) men: phylogeography of British and
587 Irish house mice. *Proceedings of the Royal Society of London B: Biological Sciences* 276:201-
588 207.
- 589 Smith AT, Xie Y. 2008. *A Guide to the Mammals of China*. Princeton, NJ: Princeton University
590 Press.
- 591 Song Y, Lan Z, Kohn MH. 2014. Mitochondrial DNA phylogeography of the Norway rat. *Plos*
592 *One* 9:e88425.
- 593 Spencer PBS, Yurchenko AA, David VA, Scott R, Koepfli K-P, Driscoll C, O'Brien SJ,
594 Menotti-Raymond M. 2016. The population origins and expansion of feral cats in Australia.
595 *Journal of Heredity* 107:104-114.

- 596 Suzuki H, Nunome M, Kinoshita G, Aplin KP, Vogel P, Kryukov AP, Jin ML, Han SH,
597 Maryanto I, Tsuchiya K, et al. 2013. Evolutionary and dispersal history of Eurasian house mice
598 *Mus musculus* clarified by more extensive geographic sampling of mitochondrial DNA. *Heredity*
599 111:375-390.
- 600 Tollenaere C, Brouat C, Duplantier J-M, Rahalison L, Rahelinirina S, Pascal M, Moné H,
601 Mouahid G, Leirs H, Cosson J-F. 2010. Phylogeography of the introduced species *Rattus rattus*
602 in the western Indian Ocean, with special emphasis on the colonization history of Madagascar.
603 *Journal of Biogeography* 37:398-410.
- 604 Waters JM. 2011. Competitive exclusion: phylogeography's 'elephant in the room'? *Molecular*
605 *Ecology* 20:4388-4394.
- 606 Weir BS, Cockerham CC. 1984. Estimating F-Statistics for the analysis of population structure.
607 *Evolution* 38:1358-1370.
- 608
- 609

610 **FIGURES**



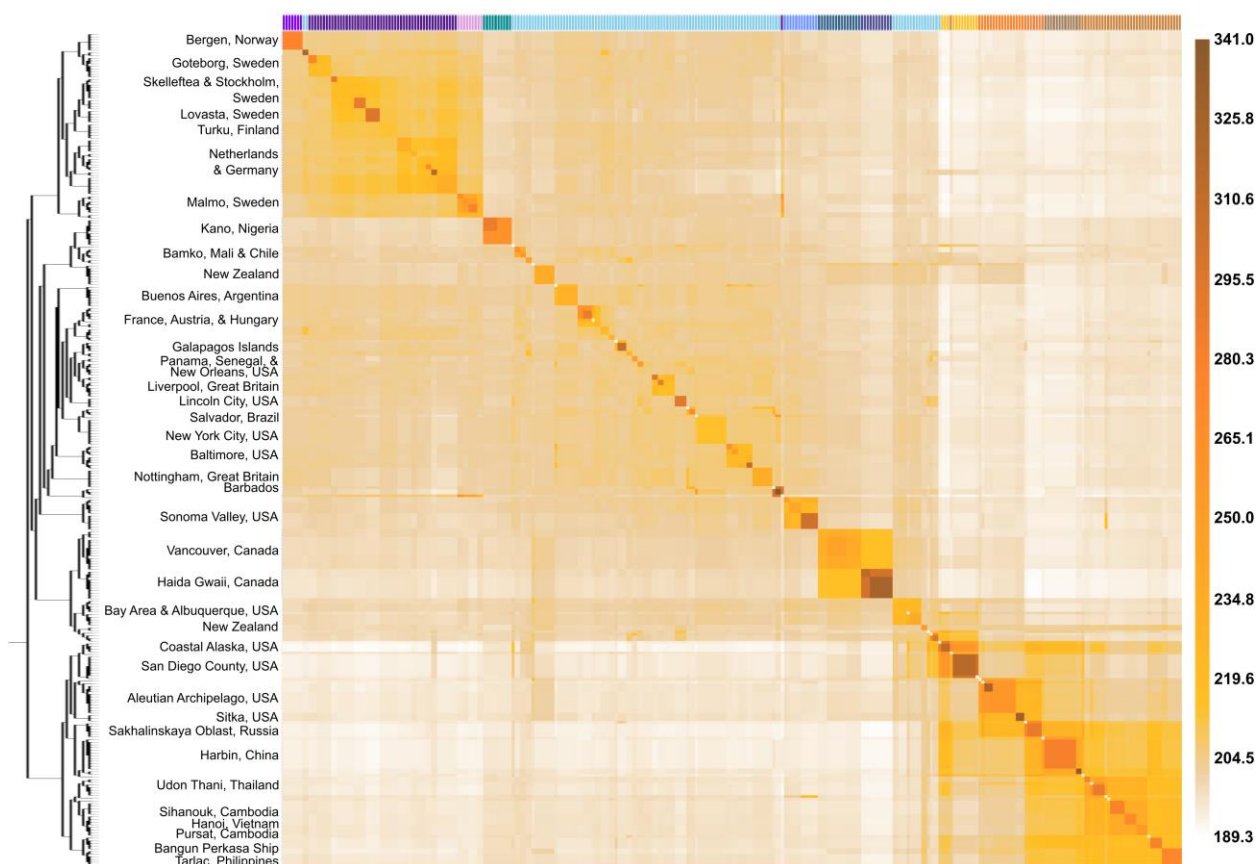
611
612 **Fig. 1-** Principal components analysis using 32k nuclear SNPs for worldwide *Rattus norvegicus*
613 samples for the first two principal components. Continents are designated by shape (Asia:
614 circles; Europe: X; Africa: star; North America: square; South America: triangle; New Zealand:
615 diamond) with substructured populations designated by color for the 13 clusters inferred using
616 model-based ancestry analyses (Figs. 2, S4).



617

618 **Fig. 2-** (A) Map of brown rat sampling locations with average proportion of ancestry per site
619 inferred using 32k nuclear SNPs. Ancestry was based on ADMIXTURE estimates from 13
620 clusters (China: brown; SE Asia: light brown; Russia: pink; Aleutian Archipelago: orange;
621 western North America: gold; W Euro: light blue; N Euro: purple; Kano: turquoise; Sonoma
622 Valley: medium blue; Haida Gwaii: dark blue; Vancouver: cerulean; Bergen: medium purple;
623 Malmo: light purple). (B) Ancestry proportions from ADMIXTURE for 314 samples at two, six,
624 13, and 26 clusters.

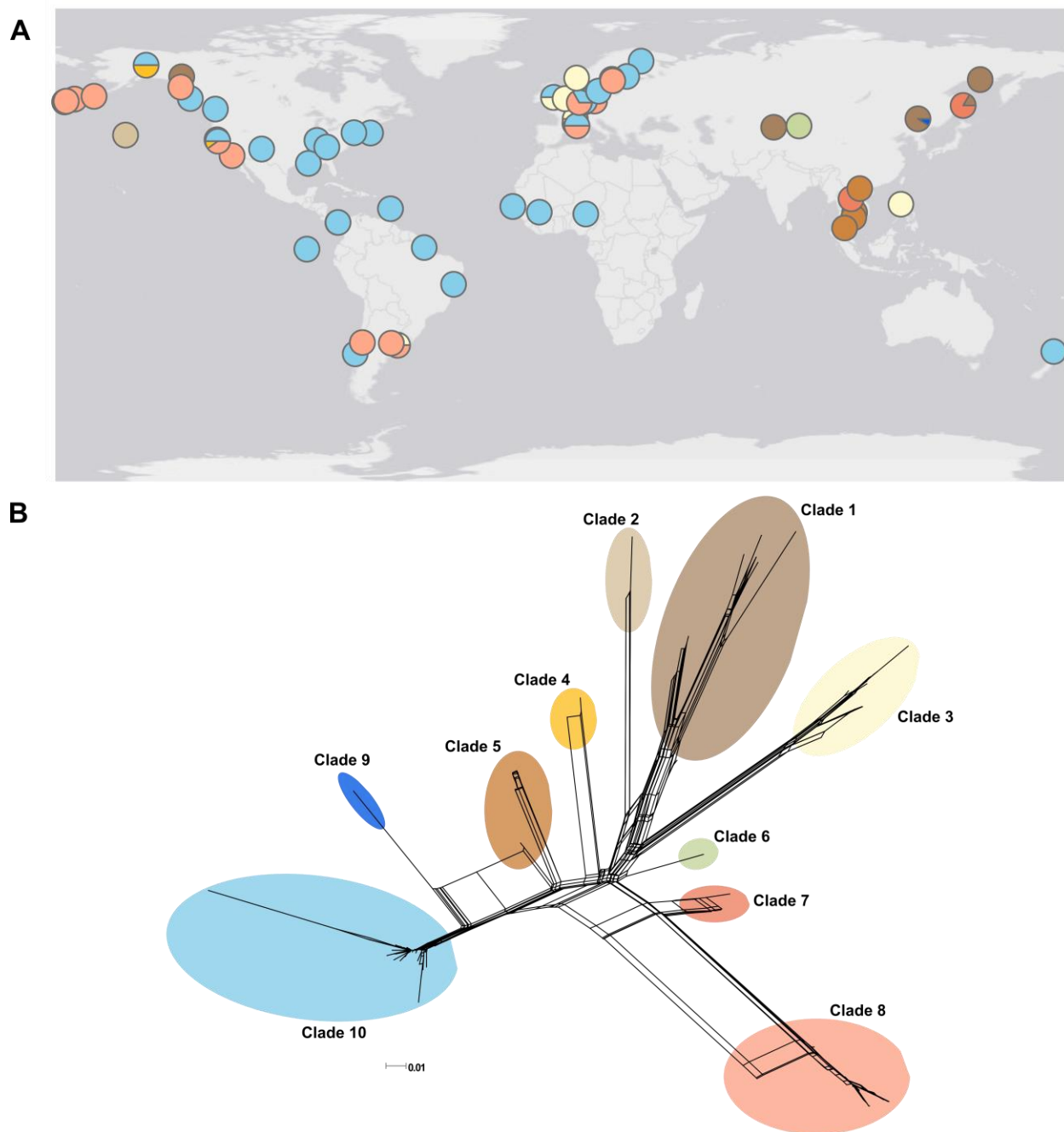
625



626

627 **Fig. 3-** Coancestry heat map of brown rats, where light and dark brown, respectively denote
628 lower and higher coancestry. The 101 populations identified by FINESTRUCTURE appear
629 along the diagonal. A bifurcating tree and select sampling locations are shown on the left, and
630 assignment to one of the 13 clusters from Fig. 2 shown on top.

631



632
633 **Fig. 4-** (A) Map of the proportion of mitochondrial clades at each sampling site for 144
634 individuals and (B) SNP haplotype network with 103 haplotypes in 10 clades (clade 1: brown; 2:
635 beige; 3: pale yellow; 4: gold; 5: light brown; 6: pale green; 7: pink; 8: light pink; 9: dark blue;
636 10: light blue).
637